Response to RC1: 'Comment on egusphere-2022-224', Anonymous Referee #1, 16 Sep 2022.
https://doi.org/10.5194/egusphere-2022-224-RC1

Comment 0. I believe this is an interesting manuscript, which will contribute to the literature on freeze/thaw classification. However, I do believe revisions are necessary before publication. I noted some more detailed points below, but in summary I believe that some additional discussions on the frequencies/angles used, and the inclusion of the other study sites as well as some discussion on the differences between the sites and the impact of this on the results would be critical.

Response to comment 0. Thank you very much, for your opinion and support. You and RC2 feedbacks gave me back the ground under my feet and the possibility of further work on the article.

Major comments:

Comment 1.

A) Line 122: "The physical basis for this effect is the observation angle of the AMSR-2 radiometer of GCOM-W1 satellite, which is close to the Brewster angle (55º)": please provide a citation(s) for this paragraph.

B) Line 98: "The difference in observation angles 40° and 55°, respectively for SMAP and AMSR2, was neglected.": why was this neglected, and what is the justification. As far as I could tell, there is no discussion on this in section 4. I believe a thorough discussion of this is necessary as this is at the basis of this methodology.

Response to comment 1.

A) AMSR2 viewing angle of 55° is very close to Brewster's angle for a natural rough surface or soil surface covered with vegetation or snow. This is not far from reality. The natural soil surface is always rough surface. If the roughness increases, Brewster's angle decreases (Ulaby, 2014, Fig. 10-17 and text on p. 437). The angle already reaches 57 degrees when roughness increases to 0.926 cm (see Fig. 10-17 below). The roughness of natural tundra soils has much higher values, which change in a wide range from 1.06 cm to 4.28 cm. (Watanabe et al., 2012).

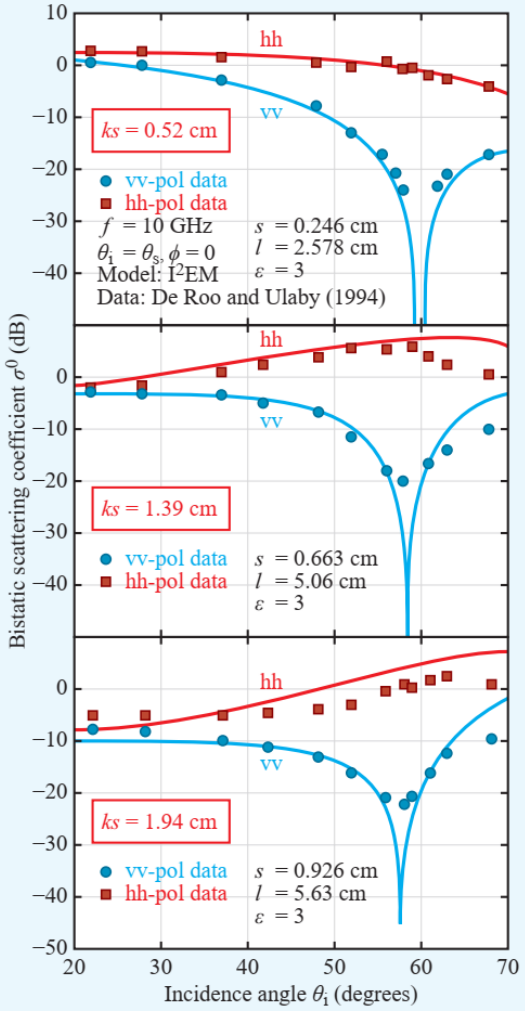

Figure 10-17: Comparison of I²EM-computed bistatic scattering coefficient with measurements made in the incidence plane ($\theta_i = \theta_s$ and $\phi = 0$) for three surfaces with different roughnesses.

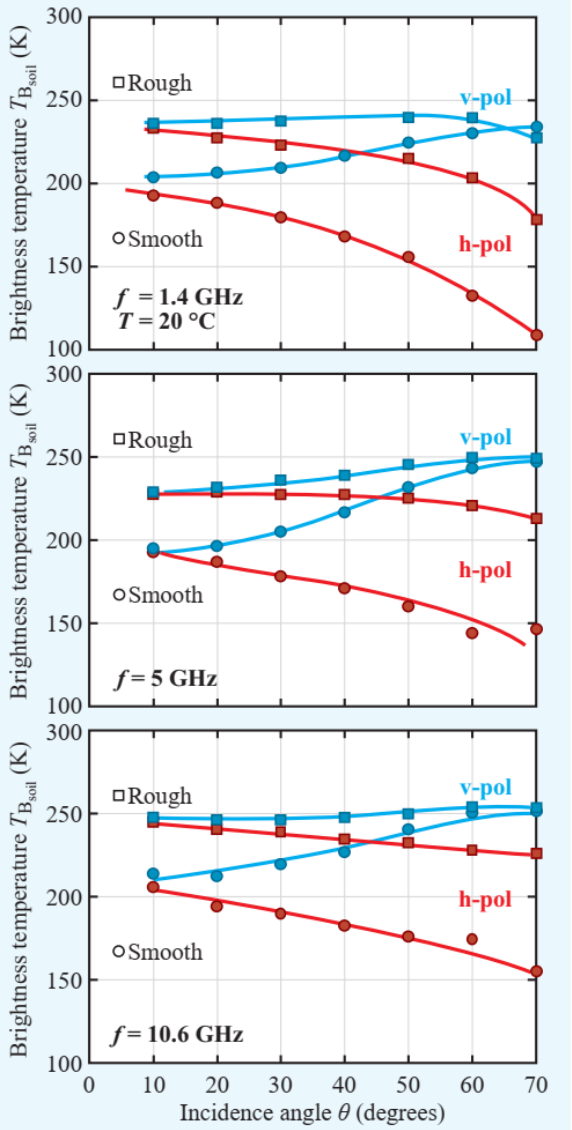

Figure 12-5: Measured brightness temperatures as a function of incidence angle at (a) 1.4 GHz, (b) 5 GHz, and (c) 10.7 GHz. The soil temperature for both smooth and rough fields was ~ 20 °C. The volumetric soil moisture content for the smooth field was ~ 0.25 g/cm^3 and for the rough field was ~ 0.26 g/cm^3 in the top 0 to 10 cm layer [Wang et al., 1983].

Reference to figures. Ulaby, F. T., Long, D. G., Blackwell, W. J., Elachi, C., Fung, A. K., Ruf, C., Sarabandi, K., Zebker, H. A., and Van Zyl, J. Microwave radar and radiometric remote sensing, University of Michigan Press Ann Arbor, MI, USA, 2014

The natural soil is covered with vegetation. As a result of interference in the canopy, the region of Brewster's angle is blurred and may contain many minimums. This can be seen, for example in (Rodriguez-Alvarez, Fig. 7, 8). Brewster's angle for vegetated soil can even be as high as 40-50° (GNSS satellite elevation) or 50-40° (in viewing angle) (Rodriguez-Alvarez, 2011, Figs. 7, 8).

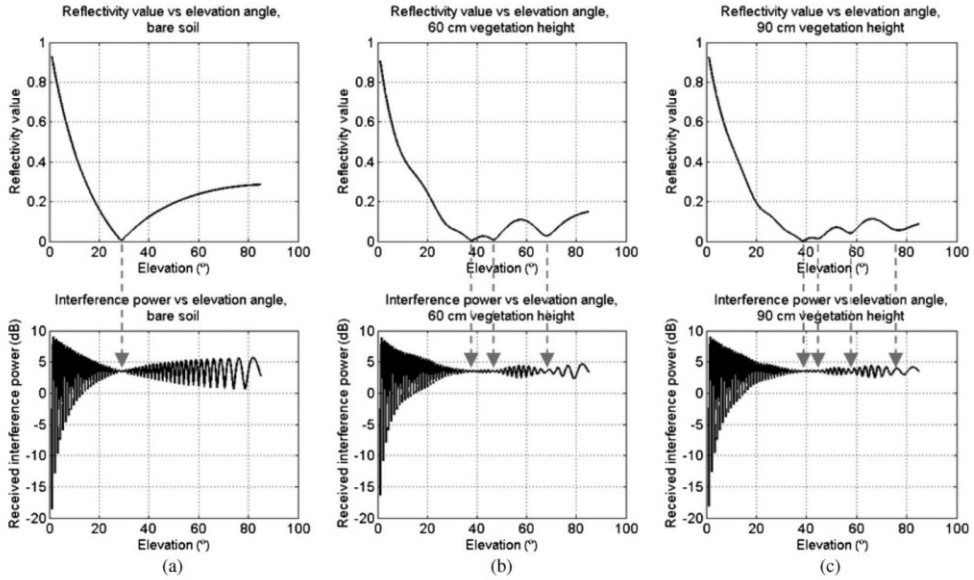

Fig. 7. Simpler model, vegetation-covered soils case. Simulated interference power received versus reflectivity. (a) Bare soil produces one notch, (b) 60-cm vegetation layer + soil layer produces three notches, and (c) 90-cm vegetation layer + soil layer produces four notches. Note that first notch is due to the Brewster's angle, but new notches appear due to oscillations in the reflectivity.

Reference to Fig.7. Rodriguez-Alvarez N. *et al*., "Land Geophysical Parameters Retrieval Using the Interference Pattern GNSS-R Technique," in *IEEE Transactions on Geoscience and Remote Sensing*, vol. 49, no. 1, pp. 71-84, Jan. 2011, doi: 10.1109/TGRS.2010.2049023.

Also, experimentally measured values of brightness temperature over thawed or frozen tundra soil (covered with snow) show that the maximum brightness temperature on vertical polarization is observed in the range of angles 45-70° (taking into account the measurement error of satellite radiometers) (Lemmetyinen et al, 2016, Fig.5-7; Ulaby et al, 2014, Fig. 12-40).

Brewster's angle is 55-65°

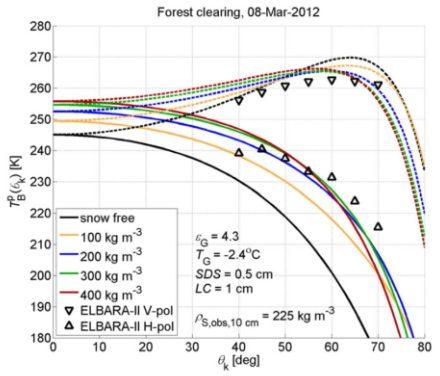

Fig. 5. Simulated (lines) and measured (symbols) L-band brightness temperatures $T_B^p(\theta_k)$ (p = H, V) as function of the incidence angle θ_k (solid lines: horizontal polarization (p = H); dashed lines: vertical polarization (p = V). Simulations using the indicated snow densities ρ_S are shown in comparison with tower-based ELBARA-II observations (triangles) performed at the forest clearing site. All simulations were made for the indicated ground permittivity ε_G and ground temperature T_G measured from SO11 sensors at 5 cm depth.

Brewster's angle is 45-55°

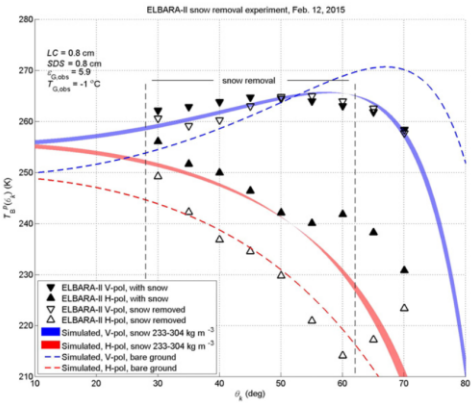

Fig. 6. Simulated (lines and shaded areas) and measured (triangles) $T_B^p(\theta_k)$ for the snow-covered footprints at the wetland site and for the corresponding footprints after snow clearing. Extent of snow clearance indicated with vertical dashed lines.

Brewster's angle are a) 60-70°, b) 55-70°, c) 55-65°, d) 55-65°

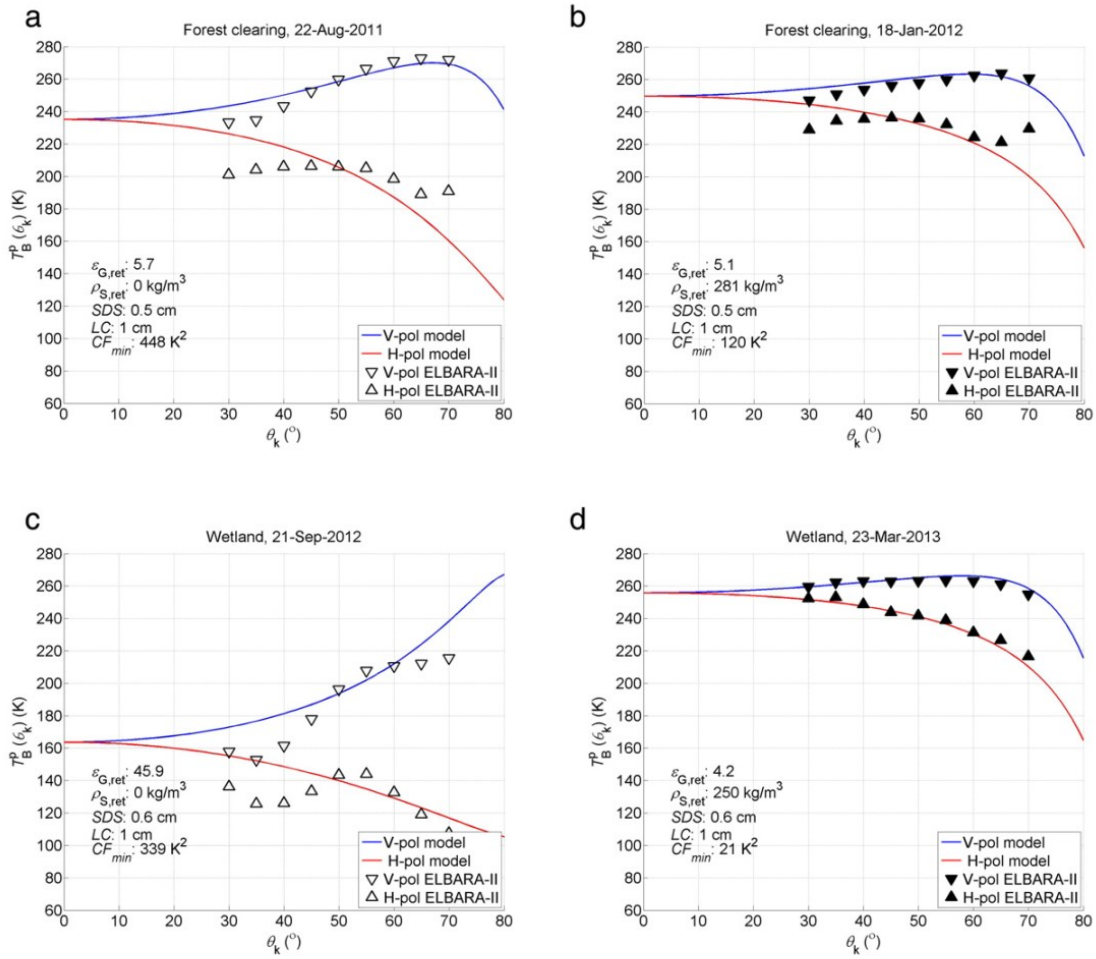

Fig. 7. Examples of simulated (lines) and observed (triangles) brightness temperatures $T_B^p(\theta_k)$ using the indicated retrieved parameters $\mathbf{P} = (\varepsilon_{G,ret}, \rho_{S,ret})$. Forest clearing site for summer (a) and winter (b); wetland site for late autumn (c) and winter (d). Observation angle ranges of $40° \le \theta_k \le 60°$ and $50° \le \theta_k \le 60°$ used for retrievals over the forest clearing and wetland sites, respectively. Hollow triangles indicate snow free conditions, filled triangles indicate presence of snow.

Reference to Fig. 7. Lemmetyinen J., Mike Schwank, Kimmo Rautiainen, Anna Kontu, Tiina Parkkinen, Christian Mätzler, Andreas Wiesmann, Urs Wegmüller, Chris Derksen, Peter Toose, Alexandre Roy, Jouni Pulliainen, Snow density and ground permittivity retrieved from L-band radiometry: Application to experimental data, Remote Sensing of Environment, Volume 180, 2016, Pages 377-391.

Brewster's angle are <40-60°

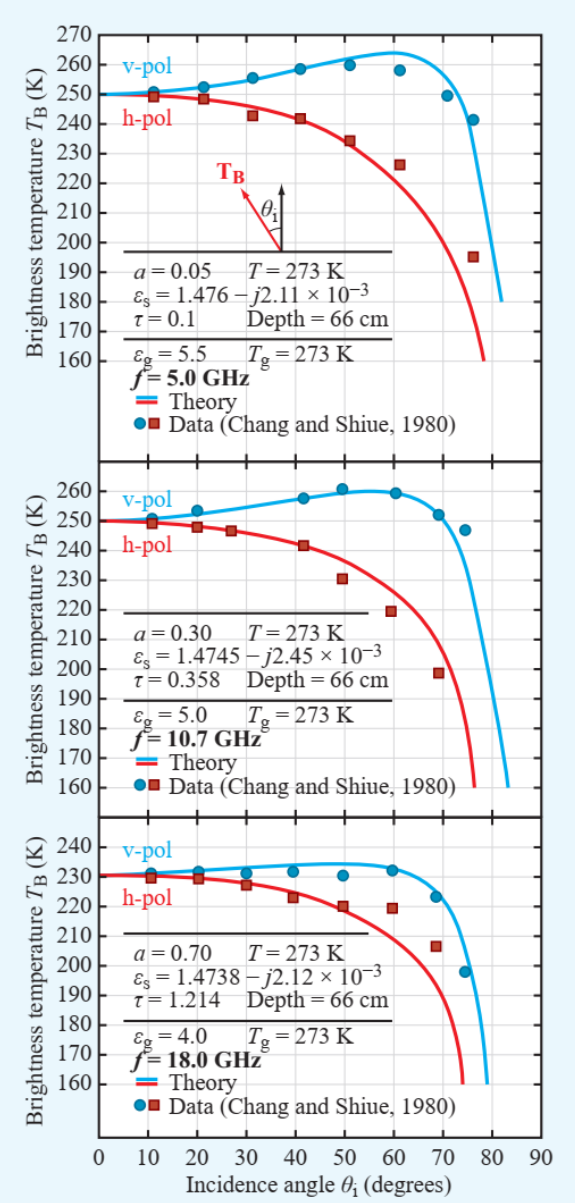

Figure 12-40: Comparison of theory with angular measurements for a snow layer with $\varepsilon_{ice} = 3.15 - j14 \times 10^{-3}$, snow density $\rho_s = 0.3$ g/cm^3, equivalent scatterer radius $r = 0.85$ mm, and wetness by weight $m_w = 0.06$ percent [Fung and Eom, 1981].

Reference to Fig. 12-40. Ulaby, F. T., Long, D. G., Blackwell, W. J., Elachi, C., Fung, A. K., Ruf, C., Sarabandi, K., Zebker, H. A., and Van Zyl, J. Microwave radar and radiometric remote sensing, University of Michigan Press Ann Arbor, MI, USA, 2014

Our calculations, which we additionally carried out for a homogeneous soil, covered with a layer of snow or vegetation, also confirm that Brewster's angle is blurred and is in the region of the AMSR2 viewing angle (see Fig. 1A, below). In the calculations, the content of organic matter in the soil was set equal to 50% (by weight), soil moisture 45% (by volume). The temperature of thawed and frozen soil was set equal to 20°C and -10°C, respectively. The soil permittivity was calculated at a frequency of 1.4 GHz based on formulas from (Mironov et al, 2019).

Reference. Mironov V. L., L. G. Kosolapova, S. V. Fomin and I. V. Savin, "Experimental Analysis and Empirical Model of the Complex Permittivity of Five Organic Soils at 1.4 GHz in the Temperature Range From −30 °C to 25 °C," in IEEE Transactions on Geoscience and Remote Sensing, vol. 57, no. 6, pp. 3778-3787, June 2019, doi: 10.1109/TGRS.2018.2887117.

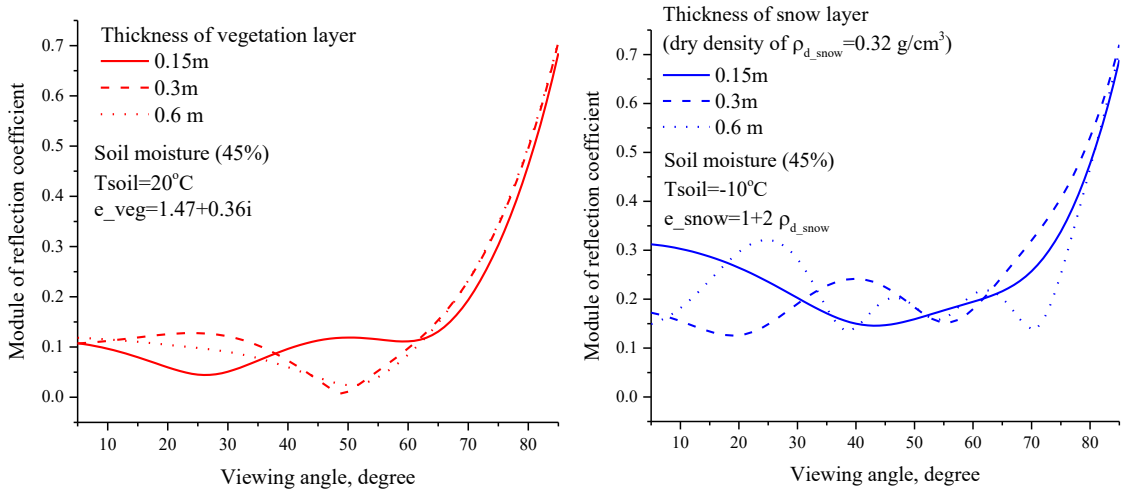

Figure 1A. Modulus of reflection coefficient (V-pol) for soil covered with vegetation (red) and snow(blue) layer. The density of dry snow was set equal to 0.32g/cm^3, and the effective permittivity of the vegetation cover was taken to be 1.47+0.36i (Schwank, 2014). **Reference.** Schwank M. et al. Model for microwave emission of a snow-covered ground with focus on L band, Remote Sensing of Environment, Volume 154, 2014, Pages 180-191

We also note the following fact. The emissivity on vertical polarization in the range of angles slightly less than Brewster's angle, weakly depends on the properties of snow canopy over soil (Schwank et al., 2014, see Fig. 9). As the snow density increases, Brewster's angle decreases and tends from 65° to ~57–50°. It can be assumed that the above results and similar conclusions are also valid when soil covered with vegetation layer.

Reference. Schwank M. et al. Model for microwave emission of a snow-covered ground with focus on L band, Remote Sensing of Environment, Volume 154, 2014, Pages 180-191.

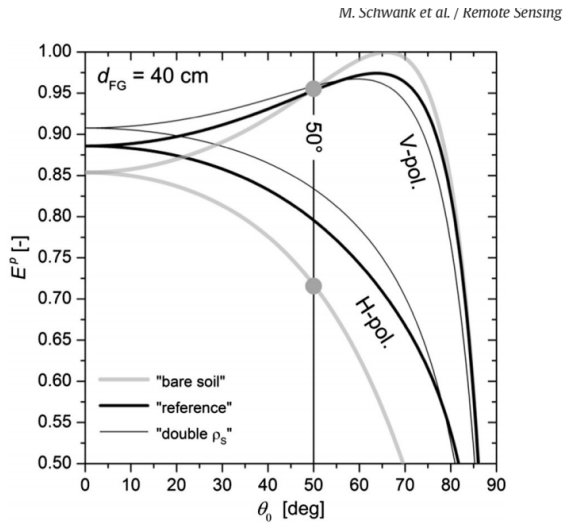

Fig. 9. Angular dependences of emissivities $E^p(\theta_0)$ of GS systems with frost-depth d_{FG} = 40 cm. Definitions of the SPs are provided in Table 2.

Reference to Fig. 9. Schwank M. et al. Model for microwave emission of a snow-covered ground with focus on L band, Remote Sensing of Environment, Volume 154, 2014, Pages 180-191. (Also see Fig. 10 in (Schwank et al, 2014).)

The analysis performed convincingly shows that the brightness temperature measured by AMSR2 at an angle of 55° is very close to the Brewster angle for a natural rough surface or soil surface covered with vegetation or snow. In addition, it should be taken into account that soils of different

moisture content, height and biomass of vegetation, different height and density of snow fall into the ~50x50 km pixel, which leads to even more blurring and smoothing of the Brewster angle area.

B) We proposed a semi-empirical approach to identify thawed and frozen states of soils. And we don't have requirements to follow mathematical rigor in formulas. We use the formulas as the main highways of radiation laws, in which, due to the empirical approach, we use brightness temperatures that do not exactly match in the sensing angle. In any case, the neglect in the sensing angle that we allowed is contained in the total error of the proposed method.

However, let us try to substantiate our assumption a little more rigorously. In accordance with expression (3) from the manuscript, when calculating

$$\Gamma_p(\theta=40°)=1-Tb_H(\theta=40°)/\ Tb_V(\theta=55°),$$

the observation angles do not coincide. $Tb_H(\theta=40°)$ measured by SMAP at 40° and $Tb_V(\theta=55°)$ measured by AMSR2/GCOM-1 at 55°. Please pay attention to emission model of ***bare*** soil (Wigneron et al., 2011), whose parameters were found on the basis of experimental data. Accuracy of the model do not better than ±4–5 K.

Reference. Wigneron J.-P., Chanzy, A., Kerr, Y., Lawrence, H. et al.: Evaluating an Improved Parameterization of the Soil Emission in L-MEB, IEEE Transactions on Geoscience and Remote Sensing, 49, 4, 1177-1189, doi: 10.1109/TGRS.2010.2075935, 2011.

In reality, soil covered with snow and vegetation within a footprint area of tens km, this error should increase significantly higher than 4-5K. Let us turn to the experimentally measured angular values of brightness temperature on horizontal and vertical polarizations over frozen and thawed tundra soil (covered and not covered with snow) (Lemmetyinen et al, 2016, Fig. 7) and soil in Canadian Prairie (Roy et al, 2018, Fig. 3)..

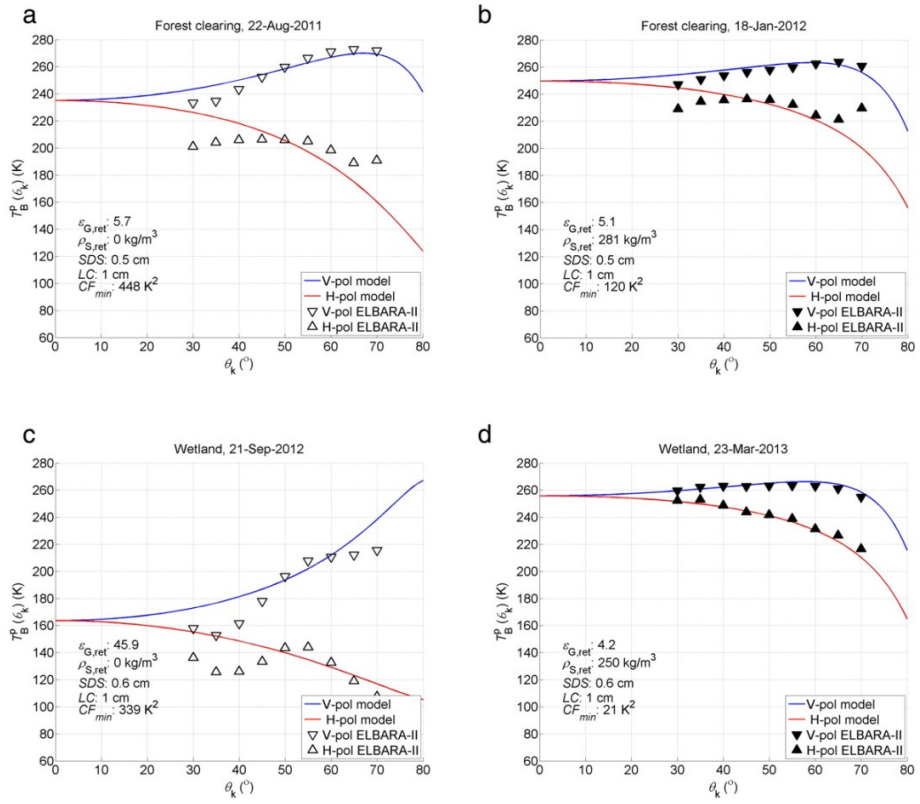

Fig. 7. Examples of simulated (lines) and observed (triangles) brightness temperatures $T_B^p(\theta_k)$ using the indicated retrieved parameters $\mathbf{P} = (\varepsilon_{G,ret}, \rho_{S,ret})$. Forest clearing site for summer (a) and winter (b); wetland site for late autumn (c) and winter (d). Observation angle ranges of $40° \le \theta_k \le 60°$ and $50° \le \theta_k \le 60°$ used for retrievals over the forest clearing and wetland sites, respectively. Hollow triangles indicate snow free conditions, filled triangles indicate presence of snow.

Reference to Fig. 7. Lemmetyinen J., Mike Schwank, Kimmo Rautiainen, Anna Kontu, Tiina Parkkinen, Christian Mätzler, Andreas Wiesmann, Urs Wegmüller, Chris Derksen, Peter Toose, Alexandre Roy, Jouni Pulliainen, Snow density and ground permittivity retrieved from L-band radiometry: Application to experimental data, Remote Sensing of Environment, Volume 180, 2016, Pages 377-391.

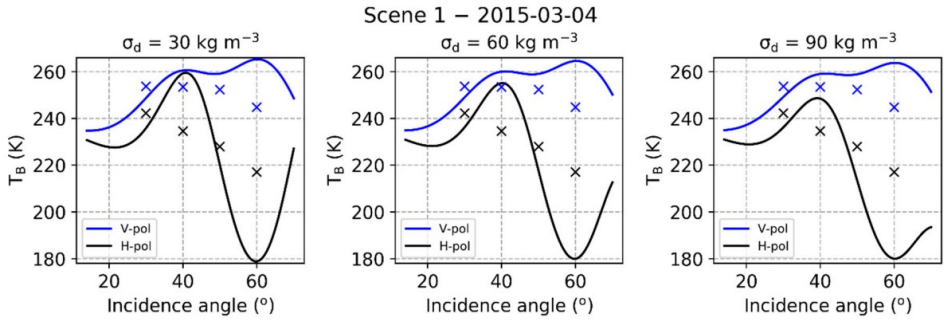

Figure 3. T_BV-pol (blue) and T_BH-pol (black) on 4 March 2015 at Scene 1 measured (symbols) and simulated (lines) with the Wave Approach for LOw-frequency MIcrowave emission in Snow (WALOMIS) with added Gaussian noise (σ_d) to the measured density of 30 kg m^{-3} (**left**), 60 kg m^{-3} (**center**) and 90 kg m^{-3} (**right**).

Reference to Fig. 3. Roy A.; Leduc-Leballeur, M.; Picard, G.; Royer, A.; Toose, P.; Derksen, C.; Lemmetyinen, J.; Berg, A.; Rowlandson, T.; Schwank, M. Modelling the L-Band Snow-Covered Surface Emission in a Winter Canadian Prairie Environment. *Remote Sens.* **2018**, *10*, 1451. https://doi.org/10.3390/rs10091451

It can be seen from the figures above that, within the error of ±5K, the angular dependence of the brightness temperature on the H-pol can be neglected within the variation of angles of 40-55°. (The exception is flooded soil, Fig. 7c). As a result, formula (3) from the manuscript can be used within the errors of measurements ±1.3-1.5 K (Piepmeier et al., 2017; Gao et al., 2019) and emission model ±4-5K (Wigneron et al., 2011)

References. Gao, S., Li, Z., Chen, Q., Zhou, W., Lin, M., Yin, X.: Inter-Sensor Calibration between HY-2B and AMSR2 Passive Microwave Data in Land Surface and First Result for Snow Water Equivalent Retrieval, Sensors, 19, 5023, doi:10.3390/s19225023, 2019.

Piepmeier, J.R., Focardi, P., Horgan, K.A., Knuble, J. et al.: SMAP L-Band Microwave Radiometer: Instrument Design and First Year on Orbit, IEEE Trans Geosci Remote Sens. 2017, 55, 4, 1954-1966, doi: 10.1109/tgrs.2016.2631978, 2017.

Wigneron J.-P., Chanzy, A., Kerr, Y., Lawrence, H. et al.: Evaluating an Improved Parameterization of the Soil Emission in L-MEB, IEEE Transactions on Geoscience and Remote Sensing, 49, 4, 1177-1189, doi: 10.1109/TGRS.2010.2075935, 2011.

In accordance with your comments in the new version of the manuscript, additional explanations are made after equation (3):

" Indeed, reflection coefficient measurements show that as root-mean-square (RMS) heights of soil surface roughness increases from 0.25 cm to 0.93 cm, Brewster's angle decreases from 60° to 57°. (De Roo and Ulaby, 1994, also see Wang et al., 1983, Fig. 2). The roughness of natural tundra soils has much higher values, which change in a wide range from 1.06 cm to 4.28 cm (Watanabe et al., 2012). The presence of vegetation (snow) cover on a rough soil surface leads to blurring and flattening of the V-pol angular dependence of reflectivity (Rodriguez-Alvarez et al., 2011, see Figs. 7, 8) and brightness temperature (Lemmetyinen et al., 2016, see Figs. 5-7; Chang and Shiue, 1980, see Fig. 3-5) in the region of Brewster's angles, due to the interference phenomenon. Within the error measurement of brightness temperature of

±1.3–1.5 K (Piepmeier et al., 2017; Gao et al., 2019), as well as the accuracy of emission models of ±4–5 K (Wigneron et al., 2011), Brewster's angle can be determined within a wide range of about from 45° to 65° (Lemmetyinen et al., 2016, see Fig. 5-7; Chang and Shiue, 1980, see Fig. 3-5). The error measurement of brightness temperature and the accuracy of emission models also makes it possible to neglect the variations of H-pol brightness temperatures of snow(vegetation)-covered soil in a range of observation angles from 40° to 55° (Roy et al., 2018, see Fig. 3; Lemmetyinen et al., 2016, see Fig. 7; Chang and Shiue, 1980, see Fig. 3-5). In this regard, the use of brightness temperatures measured at different angles in equation (3) is approximate."

Sentence: "The difference in observation angles 40° and 55°, respectively for SMAP and AMSR2, was neglected.» was delated from section 2. (The sentence in old version of the manuscript was between Line 95-100).

The list of references has been updated, see text highlighted in green in new version of manuscript.

For a more accurate understanding, proposed method, in the new version of the manuscript, we changed the notation in formula (3) for "T_{s0}" and provided links to additional literature.

Sentence

> "For an isothermal and dielectric-homogeneous half-space, the reflectivity at frequency f, in accordance with the method (Muzalevskiy and Ruzicka, 2020), can be estimated based from equation (1) assuming $\frac{\Delta T_s}{\Delta z}\Big|_{z=0} \equiv 0$:.."

was rewritten:

> "For dielectric-inhomogeneous and nonisothermal half-space, the reflectivity at frequency f, in accordance with the method (Muzalevskiy et al., 2021; Muzalevskiy and Ruzicka, 2020), can be estimated based equation:
>
> $$\Gamma_p(f) = 1 - Tb_p(f)/T_{eff}. \quad (3)$$
>
> In equation (3), T_{eff} and $\Gamma_p(f)$ can be interpreted, respectively, as effective ground-canopy temperature and ground reflectivity, which takes into account soil surface roughness and canopy optical thickness using one combined parameter (Fernandez-Moran et al., 2015, see equation (10))."

Sentence

> "The soil surface temperature T_{s0} can be estimated based on the measurements of brightness temperature $Tb_V(6.9)$ by the GCOM-W1 satellite on a frequency of 6.9 GHz in vertical polarization, the values of which correlate with the surface temperature of tundra soil (Muzalevskiy et al., 2016)."

was corrected

"The effective temperature T_{eff} can be estimated based on the measurements of brightness temperature $Tb_V(6.9)$ by the GCOM-W1 satellite on a frequency of 6.9 GHz in vertical polarization, the values of which correlate with the surface temperature of tundra soil (Muzalevskiy et al., 2016)."

References

De Roo R.D., Ulaby F.T. Bistatic specular scattering from rough dielectric surfaces. IEEE Transactions on Antennas and Propagation. 1994. V.42. №2. P. 220–231. https://doi.org/10.1109/8.277216.

Chang, A. T. C., Shiue, J. C. A comparative study of microwave radiometer observations over snowfields with radiative transfer model calculations, Remote Sensing of Environment, 10, 3, 215–229, doi:10.1016/0034-4257(80)90025-5, 1980.

Gao, S., Li, Z., Chen, Q., Zhou, W., Lin, M., Yin, X.: Inter-Sensor Calibration between HY-2B and AMSR2 Passive Microwave Data in Land Surface and First Result for Snow Water Equivalent Retrieval, Sensors, 19, 5023, doi:10.3390/s19225023, 2019.

Lemmetyinen J., Mike Schwank, Kimmo Rautiainen, Anna Kontu, Tiina Parkkinen, Christian Mätzler, Andreas Wiesmann, Urs Wegmüller, Chris Derksen, Peter Toose, Alexandre Roy, Jouni Pulliainen, Snow density and ground permittivity retrieved from L-band radiometry: Application to experimental data, Remote Sensing of Environment, Volume 180, 2016, Pages 377-391.

Piepmeier, J.R., Focardi, P., Horgan, K.A., Knuble, J. et al.: SMAP L-Band Microwave Radiometer: Instrument Design and First Year on Orbit, IEEE Trans Geosci Remote Sens. 2017, 55, 4, 1954-1966, doi: 10.1109/tgrs.2016.2631978, 2017.

Rodriguez-Alvarez N. et al., "Land Geophysical Parameters Retrieval Using the Interference Pattern GNSS-R Technique," in IEEE Transactions on Geoscience and Remote Sensing, vol. 49, no. 1, pp. 71-84, Jan. 2011, doi: 10.1109/TGRS.2010.2049023.

Roy A.; Leduc-Leballeur, M.; Picard, G.; Royer, A.; Toose, P.; Derksen, C.; Lemmetyinen, J.; Berg, A.; Rowlandson, T.; Schwank, M. Modelling the L-Band Snow-Covered Surface Emission in a Winter Canadian Prairie Environment. Remote Sens. 2018, 10, 1451. https://doi.org/10.3390/rs10091451

Watanabe M. et al., "Analysis of the Sources of Variation in L-band Backscatter From Terrains With Permafrost," in IEEE Transactions on Geoscience and Remote Sensing, vol. 50, no. 1, pp. 44-54, Jan. 2012, doi: 10.1109/TGRS.2011.2159843.

Wigneron J.-P., Chanzy, A., Kerr, Y., Lawrence, H. et al.: Evaluating an Improved Parameterization of the Soil Emission in L-MEB, IEEE Transactions on Geoscience and Remote Sensing, 49, 4, 1177-1189, doi: 10.1109/TGRS.2010.2075935, 2011.

Comment 2. Figure 1: Only Happy Valley test site is shown. I would argue its critical to somehow show the other test sites as well. At the very least there should be an example of one of the sites where the methodology does not work as well according to the authors.

Response to comment 2. We proceeded from the limited volume of the article. In accordance with your comment, we have added to Fig. 2 dependences $\Delta\Gamma_H(f)/\Delta f$ for test sites of KJ, CH, including SO, SA. In these areas, from our point of view, the method is quite suitable for use, the method reflects the objective situation of soil surface temperature fluctuations near 0C (please see response to comment 3 below). Contrary to the manuscript, below are figures for both $\Delta Tb_H(f)/\Delta f$ and $\Delta\Gamma_H/\Delta f$ for several test sites. Additional discussion of the new figures is provided in the response to comment 3 (see below).

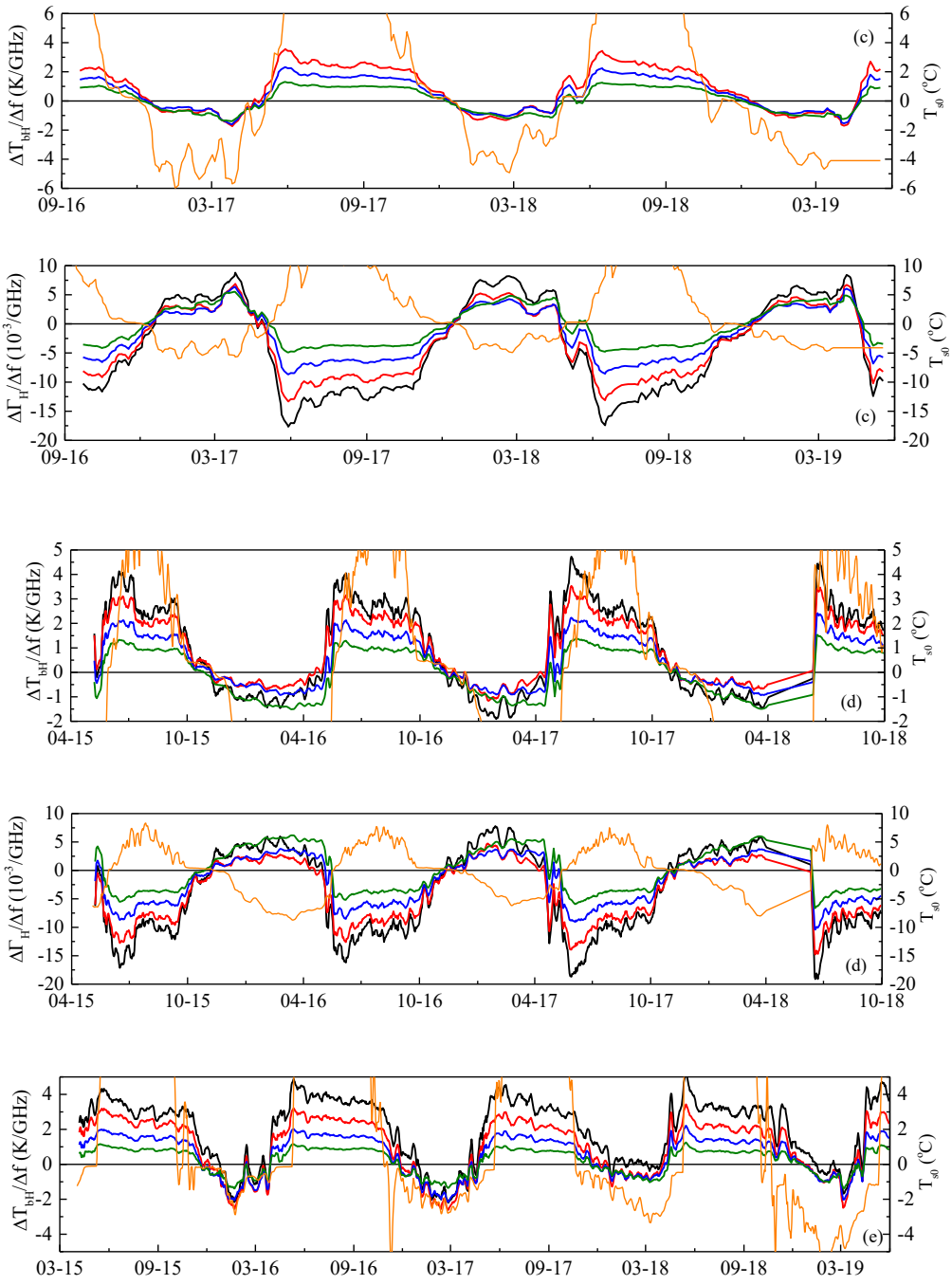

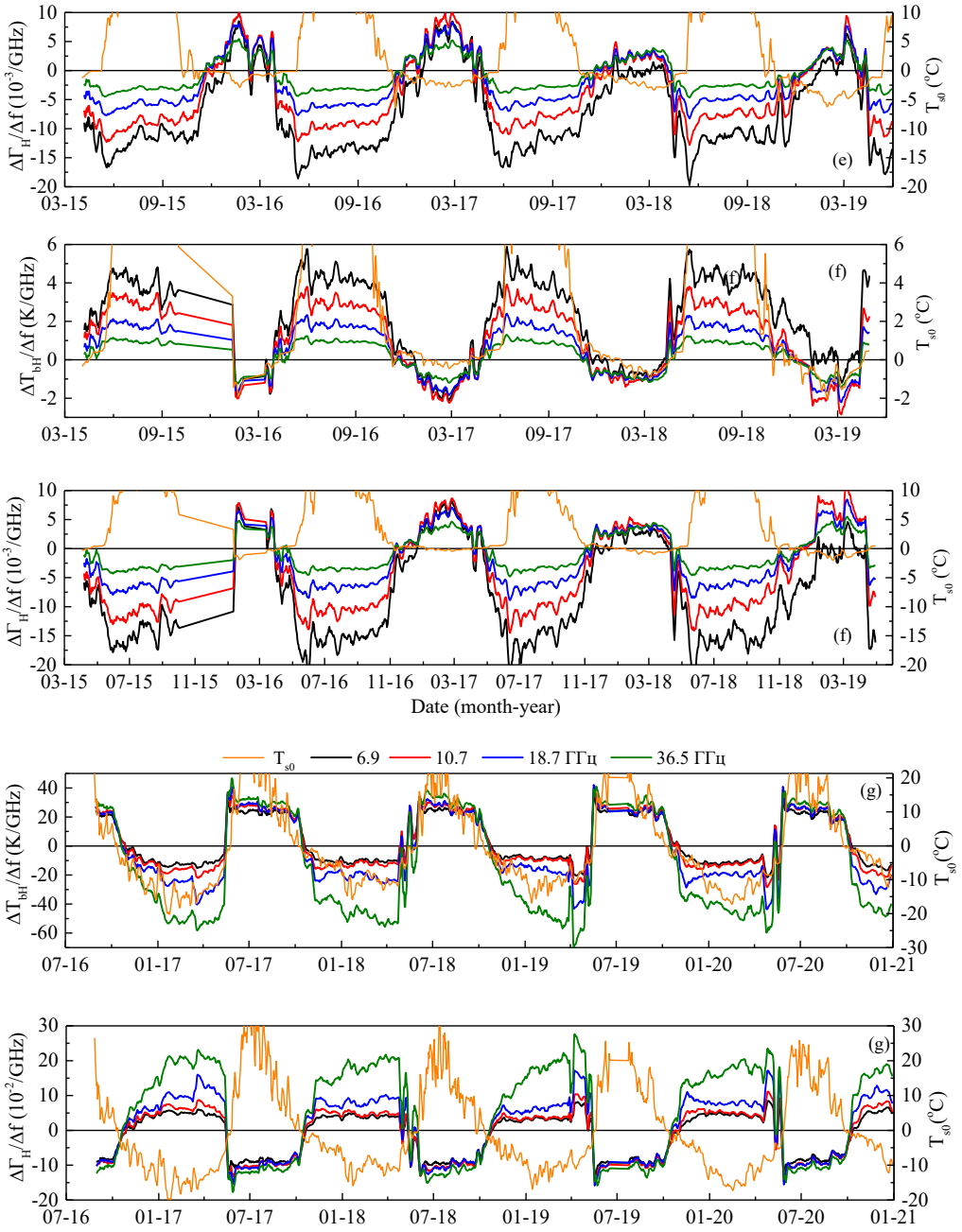

Fig. 1. (Fig. 2 in manuscript). Test sites:(c) KJ, (d) CH, (e) SO, (f) SA, (g) FB

Caption to Fig. 2 in the new version of the manuscript was changed to:

" Figure 2. Density of spectral gradients of brightness temperature (a) and reflectivity (b) for HV test site, and density of spectral gradients of reflectivity for (c) KJ, (d) CH, (e) SO, (f) SA test sites, calculated for the pairs of frequencies: 1) 1.4-6.9 GHz, 2) 1.4-10.7 GHz, 3) 1.4-18.7 GHz and 4) 1.4-36.5 GHz."

Comment 3.

In section 2, the authors describe differences and similarities between the test sites. I can not see any discussion on how those conditions influence the outcome except for 'surface water area' which is briefly discussed but not with a focus on the differences between test sites. Please elaborate in the discussion section the soundness of the results for those different sites as it speaks to the transferability of your approach.

Line 181-182: Does this mean that this method is not applicable in lower latitudes/sub Arctic regions? Please expand/clarify.

Response to comment 3. In accordance with the comment, we had made further discussions. In the paragraph before Fig. 2 the following sentences have been added:

> "Similar patterns in the behavior of $\Delta Tb_H(f)/\Delta f$ and $\Delta\Gamma_H(f)/\Delta f$ are also observed for other test sites, except SO and SA. As an example, $\Delta\Gamma_H(f)/\Delta f$ for KJ, CH, SO, and SA test sites are shown in Fig. 2c-2f. In some years, for SO and SA test sites, multiple passing of $\Delta\Gamma_H(f)/\Delta f$ through 0 during winter can be observed (see Fig. 2e, 2f), which does not allow unambiguous identification of FT soil states. These processes will be explained below. Also note, in comparison with other test sites, the presence of significant wetland and open water at the CH test site (see Table 1) is not detected in the behavior of $\Delta\Gamma_H(f)/\Delta f$ ($\Delta Tb_H(f)/\Delta f$)."

The following paragraph has been added at the end of section 4:

> "This systematic error may be because, in contrast to the other test sites, SO and SA stand out by the largest share of a forest, from 70% to 85% in the footprint (see Table 1). Apparently, such a significant share of forests contributes to the formation of a thicker forest litter and increased accumulation of snow cover compared to the rest test sites, as well as to the test sites KJ and CH, the share of forests in which is less (60% and 53%, respectively). More thick forest litter and snow cover create additional inertia in the thermal exchange between air and soil. Indeed, according to SO and SA stations data, these test sites have characteristics of small negative soil surface temperatures in winter, as well as the extended period of zero-curtain effect (see Fig. 2e, 2f). As a result, in some years, the unstable-transition FT soil state is reflected in the unstable transition of $\Delta\Gamma_H(f)/\Delta f$ ($\Delta Tb_H/\Delta f$) through 0 during winter, which explains the observed systematic error on SO and SA test sites. Similar unstable transitions of brightness temperature have been observed in ground-based radiometric experiments at the SO test site (Lemmetyinen et al., 2016, see Fig. 2 "wetland 2013-2014"); as well thawed soil under dry snow layer is a common phenomenon (Kumawat et al., 2022)."

In the "Conclusion" section, sentences was added:

> "The proposed method makes it possible to identify forest soils are in a transitional state (the soil surface temperature is about 0°C or has small negative values), which is revealed in the multiple transitions of spectral gradient densities of brightness temperature and reflectivity through 0 (more pronounced in the frequency range of 1.4-6.9 GHz)..... We did not find any significant differences in the behavior of the spectral gradient densities of brightness temperature and reflectivity, measured for the test site with a high share of wetland (20%) and open water (19%) from the other test sites..."

Sentence

The last sentences in "Conclusion"

> "If we neglect the influence of water bodies (with less than 19% of the total pixel area), then, as shown in this work, FT topsoil state identification is possible with determination coefficient of 0.775-0.834, root-mean-square-error of 6.6-10.7 days, and bias from -3.4 to +6.5 days."

was rewritten:

> "Despite all assumptions made in the proposed method, the identification of FT soil surface states is possible with a relatively high determination coefficient of 0.775-0.834, small root-mean-square-error of 6.6-10.7 days, and bias from -3.4 to +6.5 days."

References

Lemmetyinen, J., Schwank, M., Rautiainen, K., Kontu, A., Parkkinen, T., Mätzler, C., Wiesmann, A., Wegmüller, U., Derksen, C., Toose, P., Roy, A., Pulliainen, J.: Snow density and ground permittivity retrieved from L-band radiometry: application to experimental data, Remote Sensing of Environment, 180, 377-391, 10.1016/j.rse.2016.02.002, 2016.

Kumawat, D., Olyaei, M., Gao, L., Ebtehaj, A.: Passive Microwave Retrieval of Soil Moisture Below Snowpack at L-Band Using SMAP Observations, IEEE Transactions on Geoscience and Remote Sensing, 60, 4415216, 1-16, doi: 10.1109/TGRS.2022.3216324, 2022.

Minor comments:

Comment 4. Line 134: ovals are not visible possibly replace with vertical line with a stronger color/stronger line width.

Response to comment 4. Fig.1a, 1b were replaced. In the new version of the manuscript the selected areas are shown as rectangles with a dash line. In the new version of the manuscript word “ovals” was replaced to “rectangles” on

Line 145: “Several such time periods are marked by rectangles with a dashed line in Fig. 1a, 1b (see the period 2015-2016). ”

Comment 5. Figure 3: Figure caption to long, difficult to get the essential points from it. Please shorten. Also, it should be made clear in the figure caption that the different colors represent the different test sites.

Response to comment 5. Caption to Fig. 3 was replaced to

> "Correlation between days of the year (DoY), for which: (a) $\Delta Tb_H/\Delta f$, (b) $\Delta \Gamma_H/\Delta f$, (c) MPR crosses threshold level, (d) FT soil state was detected (SMAP SPL3FTP_E product) and soil surface temperature stable crossing 0°C (weather stations data). Different test sites are marked with color symbols. The open and filled symbols indicate the frozen and thawed surface soil state, respectively. Squares and circles (regression lines) correspond to the spectral range of 6.9-1.4 GHz (1) and 36.5-1.4 GHz (2), respectively. Regression line (3) corresponds to MPR index and SMAP SPL3FTP_E product."

Comment 6. Line 188: swap identification with identify

Response to comment 6. Done.

Comment 7. Line 198: "FT topsoil state identification possible with determination coefficient": missing 'is'

Response to comment 7. Verb was inserted in sentence.

Comment 8. The word 'region' is used several times incorrectly in my opinion. Specifically, line 138 where it should be replaced by 'time period' or something similar.

Response to comment 8. It was corrected.

Sentence before Fig. 1 was corrected:

> "Several such time periods are marked by rectangles with a dashed line in Fig. 1a, 1b (see the period 2015-2016)."

Sentence after Fig. 1 was corrected:

> "In the transition period (May 7-19, 2016 and October-November, 2015, see Fig. 1)...."